SUPERCONDUCTIVITY WS 15-16

Monday 10:00-11:30

SR Exp. physics II

Prof. Paul H.M. van Loosdrecht

pvl@ph2.uni-koeln.de

www.loosdrecht.net

- New record BCS superconductivity

- Optical induced superconductivity

Direct observation of an abrupt insulator-to-metal transition in dense liquid deuterium

M. D. Knudson,[1]* M. P. Desjarlais,[1] A. Becker,[2] R. W. Lemke,[1] K. R. Cochrane,[1] M. E. Savage,[1] D. E. Bliss,[1] T. R. Mattsson,[1] R. Redmer[2]

Eighty years ago, it was proposed that solid hydrogen would become metallic at sufficiently high density. Despite numerous investigations, this transition has not yet been experimentally observed. More recently, there has been much interest in the analog of this predicted metallic transition in the dense liquid, due to its relevance to planetary science. Here, we show direct observation of an abrupt insulator-to-metal transition in dense liquid deuterium. Experimental determination of the location of this transition provides a much-needed benchmark for theory and may constrain the region of hydrogen-helium immiscibility and the boundary-layer pressure in standard models of the internal structure of gas-giant planets.

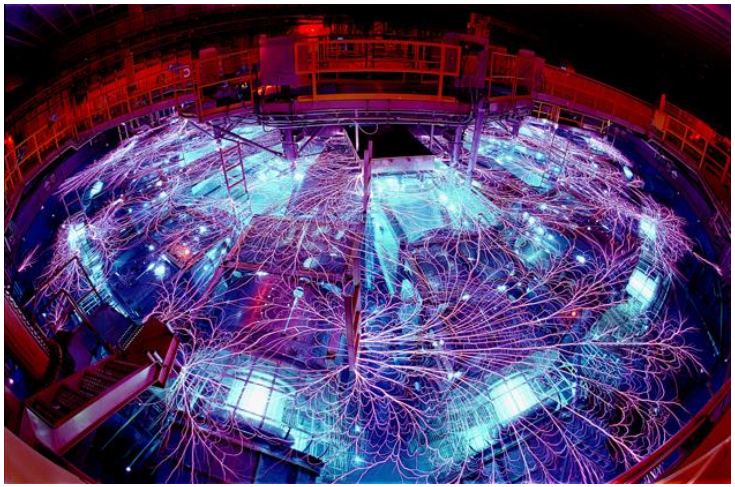

In 1935, Wigner and Huntington (*1*) were the first to predict that when squeezed to sufficiently high density (ρ) and pressure (*P*), hydrogen would undergo a density-driven transition from an insulating, molecular solid to a conducting, atomic solid. Subsequently, this fundamental question of precisely how and at what *P* hydrogen metallizes at low temperature (*T*) has become one of the longest-standing open questions of high-pressure physics (*2*). More recently, there has been much interest in the analogous molecular insulator to atomic metal transition in the liquid at low *T* just above the melt line, largely due to its relevance to planetary science (*3*, *4*). A metallization transition in this region could provide a constraint for the

[1]Sandia National Laboratories, Albuquerque, NM, USA. [2]Institute of Physics, University of Rostock, Rostock, Germany.
*Corresponding author. E-mail: mdknuds@sandia.gov

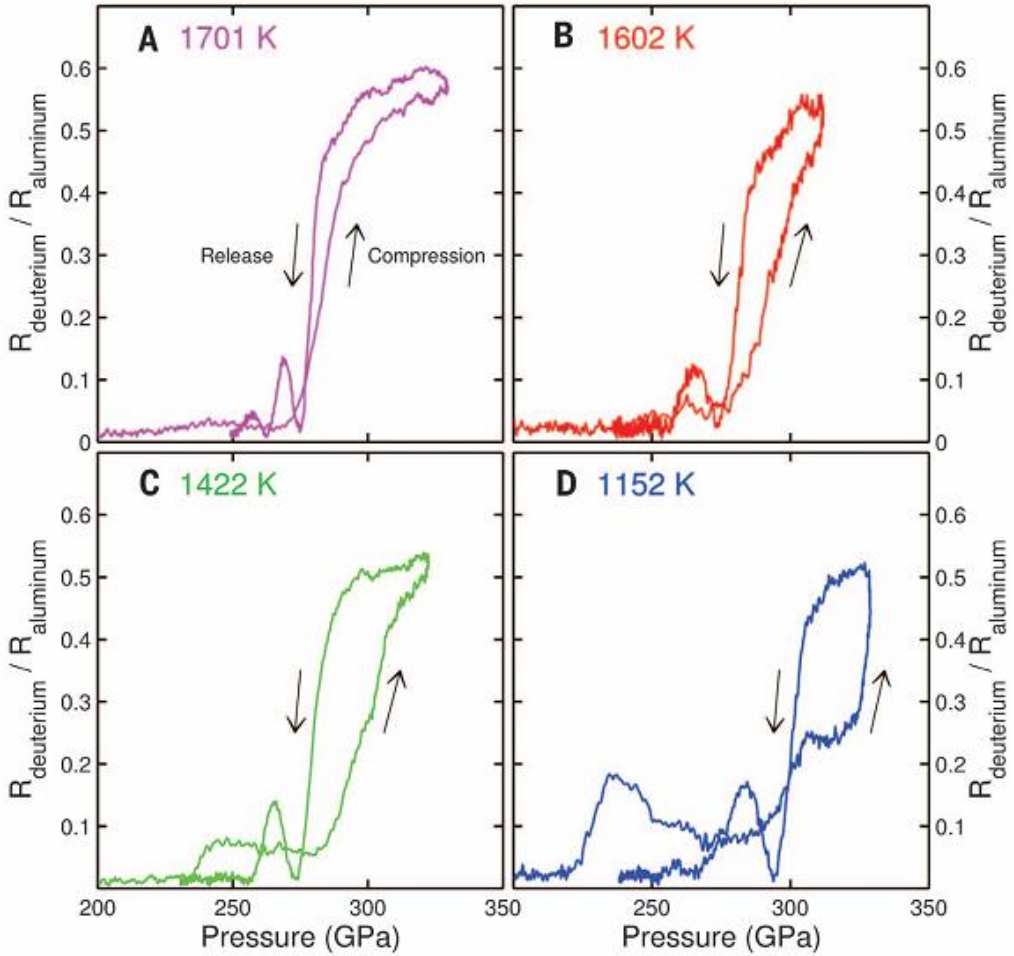

Fig. 4. Reflectivity versus *P*. Measured deuterium reflectivity with respect to aluminum reflectivity (from the interferometer) versus *P* for each experiment. (**A** to **D**) denote the highest- to lowest-*T* experiments, respectively. Colors correspond to the *PT* paths displayed in Fig. 1. *T* indicated in each panel corresponds to the estimated *T* at the phase boundary, neglecting any latent heat. All experiments show an asymmetry in the deuterium reflectivity with *P*; the drop in reflectivity upon *P* release is considerably sharper than the increase in reflectivity upon compression. This asymmetry, which is more pronounced at lower *T*, is likely due to the effects of thermal conduction (*18*). All experiments also show a small but measurable reflectivity that precedes the abrupt reflectivity increase, which again is more pronounced at lower *T*. Finally, all experiments show oscillatory behavior of the reflectivity upon further release of *P* below the IMT boundary.

LETTER

doi:10.1038/nature14964

Conventional superconductivity at 203 kelvin at high pressures in the sulfur hydride system

A. P. Drozdov[1]*, M. I. Eremets[1]*, I. A. Troyan[1], V. Ksenofontov[2] & S. I. Shylin[2]

A superconductor is a material that can conduct electricity without resistance below a superconducting transition temperature, T_c. The highest T_c that has been achieved to date is in the copper oxide system[1]: 133 kelvin at ambient pressure[2] and 164 kelvin at high pressures[3]. As the nature of superconductivity in these materials is still not fully understood (they are not conventional superconductors), the prospects for achieving still higher transition temperatures by this route are not clear. In contrast, the Bardeen–Cooper–Schrieffer theory of conventional superconductivity gives a guide for achieving high T_c with no theoretical upper bound—all that is needed is a favourable combination of high-frequency phonons, strong electron–phonon coupling, and a high density of states[4]. These conditions can in principle be fulfilled for metallic hydrogen and covalent compounds dominated by hydrogen[5,6], as hydrogen atoms provide the necessary high-frequency phonon modes as well as the strong electron–phonon coupling. Numerous calculations support this idea and have predicted transition temperatures in the range 50–235 kelvin for many hydrides[7], but only a moderate T_c of 17 kelvin has been observed experimentally[8]. Here we investigate

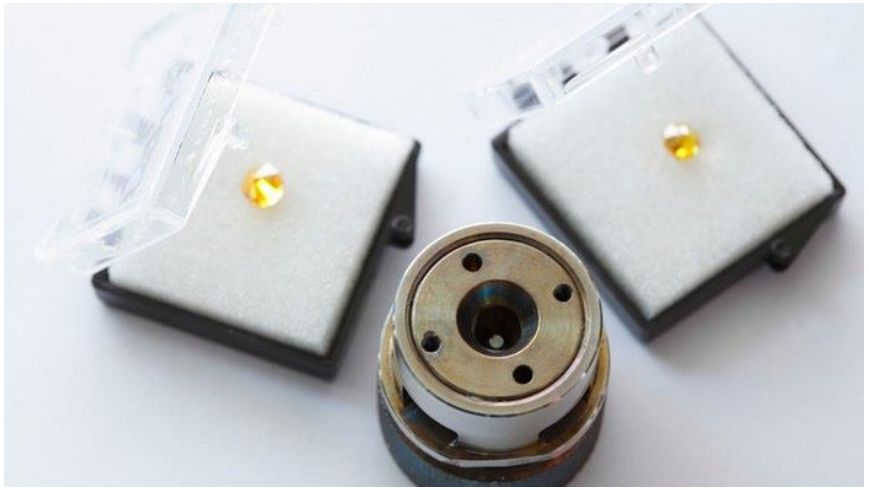

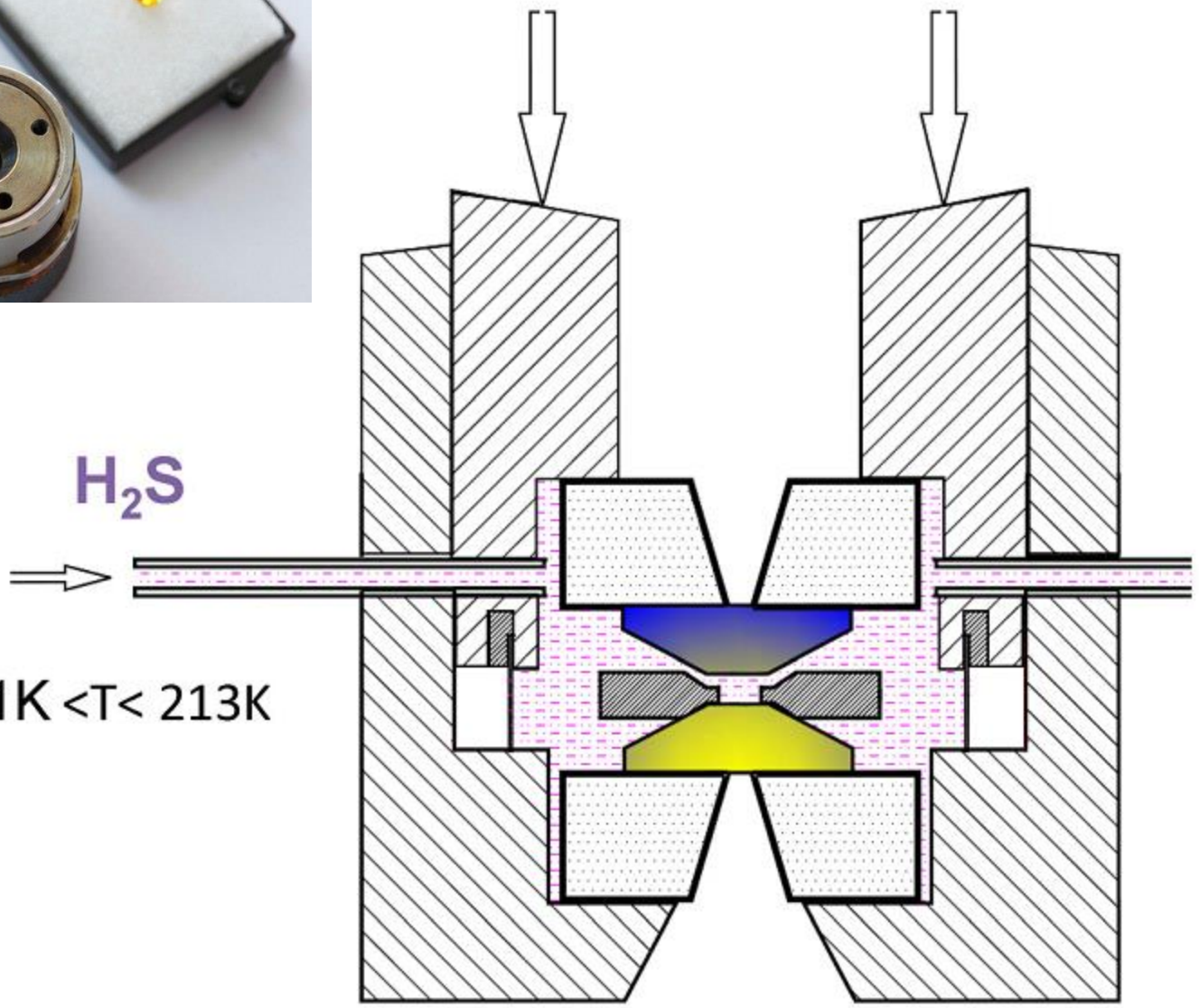
H_2S
191K <T< 213K

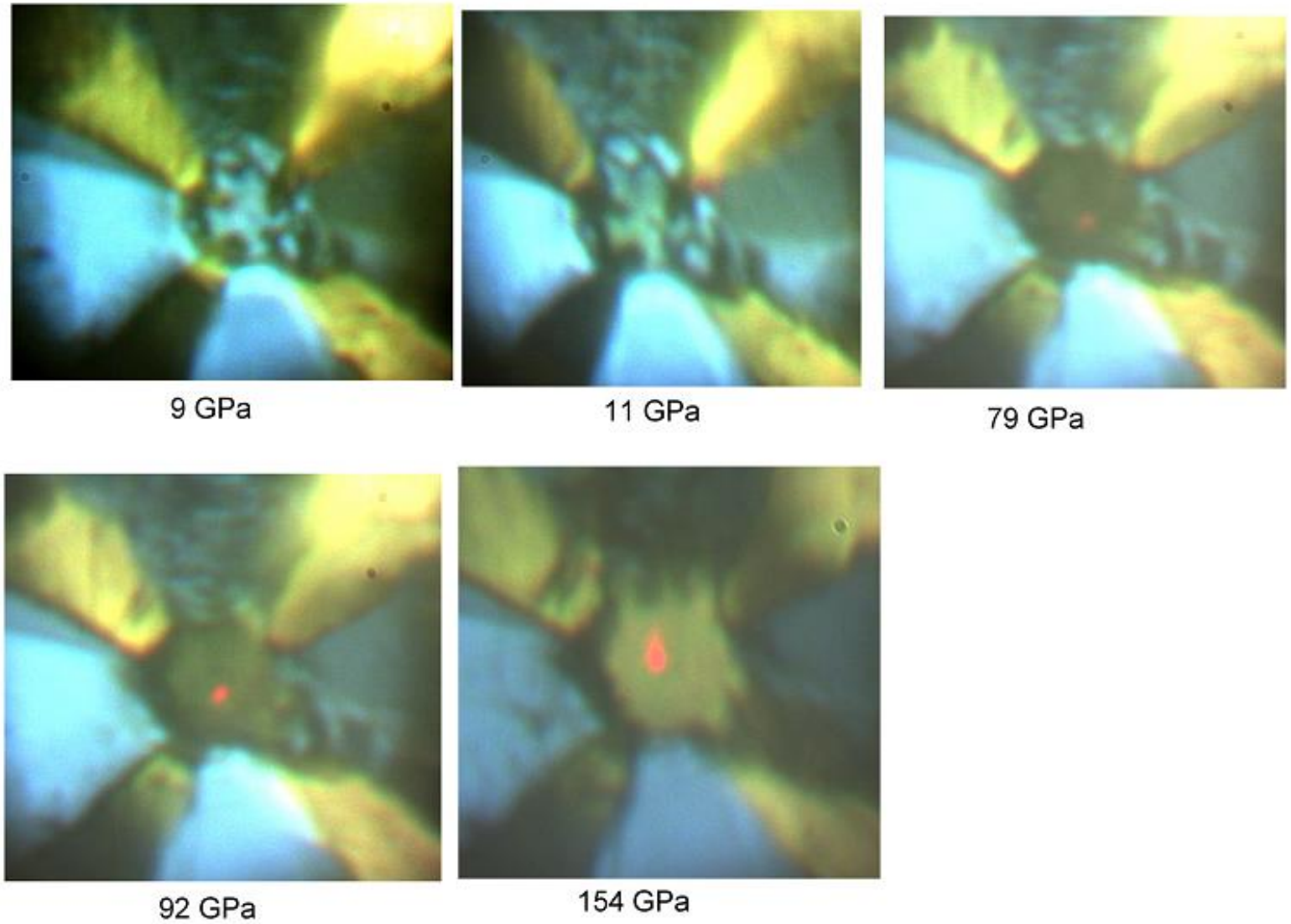

Extended Data Figure 5 | View of D_2S sample with electrical leads and transparent gasket ($CaSO_4$) at different pressures. The D_2S is in the centre of these photographs, which were taken in a cryostat at 220 K with mixed illumination, both transmitted and reflected. Under this illumination, the insulating transparent gasket shows blue, and the electrodes yellow. The red spot is the focused HeNe laser beam. The sample, which is initially transparent, becomes opaque and then reflective as pressure is increased.

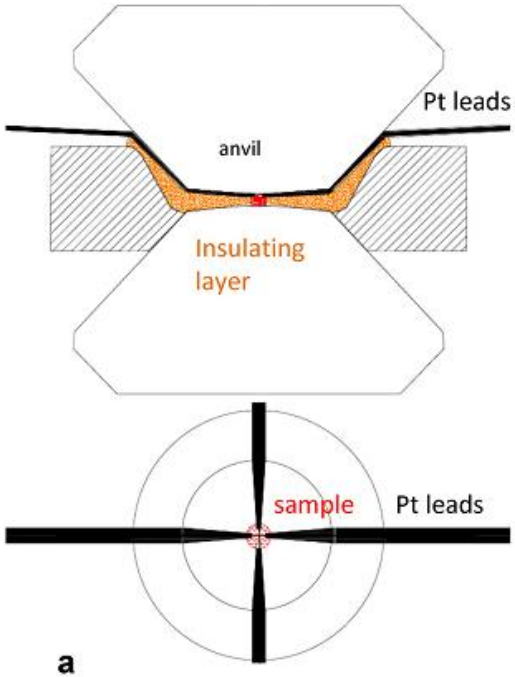

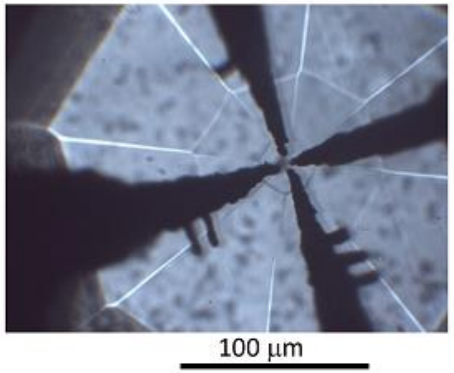

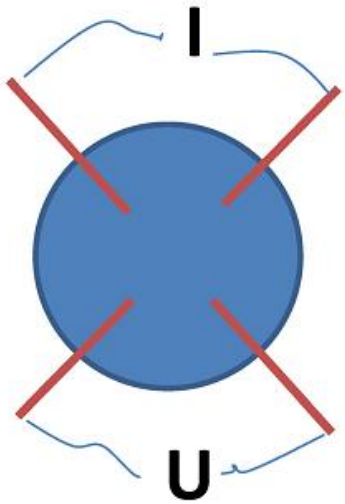

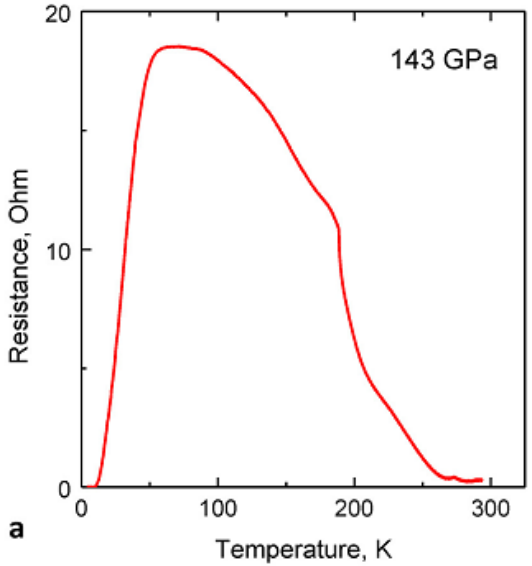

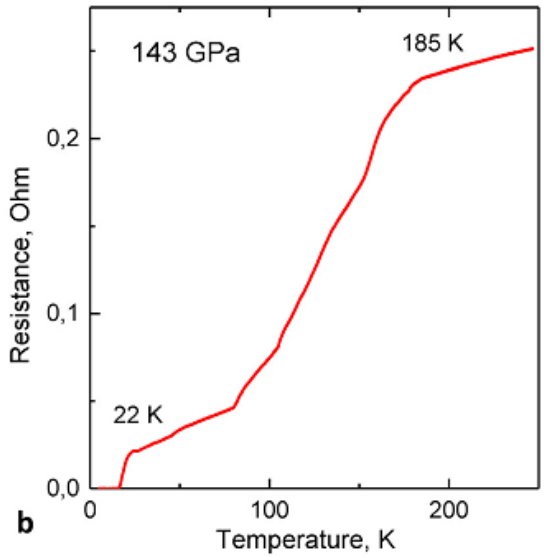

Extended Data Figure 2 | Temperature dependence of the resistance of sulfur hydride at 143 GPa. In this run the sample was clamped in the DAC at $T \approx 200$ K, and the pressure then increased to 103 GPa at this temperature; the further increase of pressure to 143 GPa was at ~100 K. **a**, After next cooling to ~15 K and subsequent warming, a superconducting transition with $T_c \approx 60$ K was observed, then the resistance strongly decreased with increasing temperature. After successive cooling and warming (**b**; only the warming curve is shown) a kink at 185 K appeared, indicating the onset of superconductivity. The superconducting transition is very broad: resistance dropped to zero only at ~22 K. There are apparent 'oscillations' on the slope. Their origin is not clear, though they probably reflect inhomogeneity of the sample in the transient state before complete annealing. Similar 'oscillations' have also been observed for other samples (see, for example, figure 3 in the Supplementary Information of ref. 9).

Zero resistance

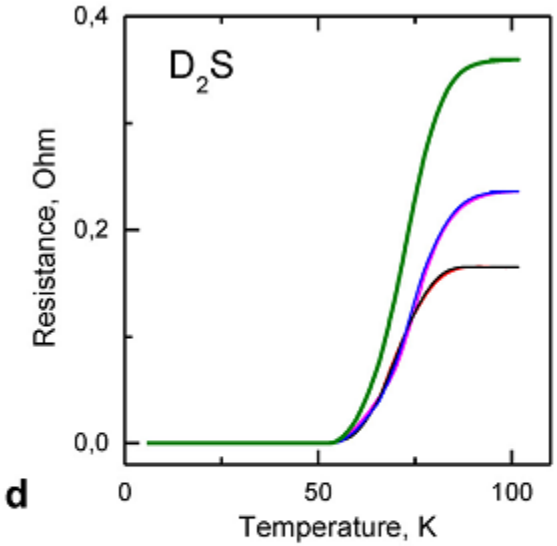

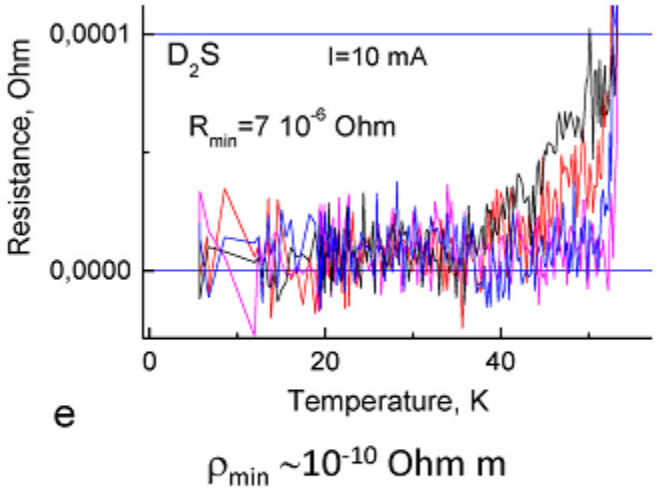

ρ_{min} ~10^{-10} Ohm m

Extended Data Figure 3 | Electrical measurements. **a**, Schematic drawing of diamond anvils with electrical leads separated from the metallic gasket by an insulating layer (shown orange). **b**, Ti electrodes sputtered on a diamond anvil shown in transmitted light. **c**, Scheme of the van der Pauw measurements: current leads are indicated by *I*, and voltage leads as *U*. **d**, Typical superconducting step measured in four channels (for different combinations of current and voltage leads shown in **c**). A sum resistance obtained from the van der Pauw formula is shown by the green line. Note here that the superconducting transition was measured with the un-annealed sample[9]. After warming to room temperature and successive cooling, T_c should increase. **e**, Residual resistance measured below the superconducting transition (**d**). R_{min} and ρ_{min} are averaged over four channels shown by different colours.

Field dependence, critical field

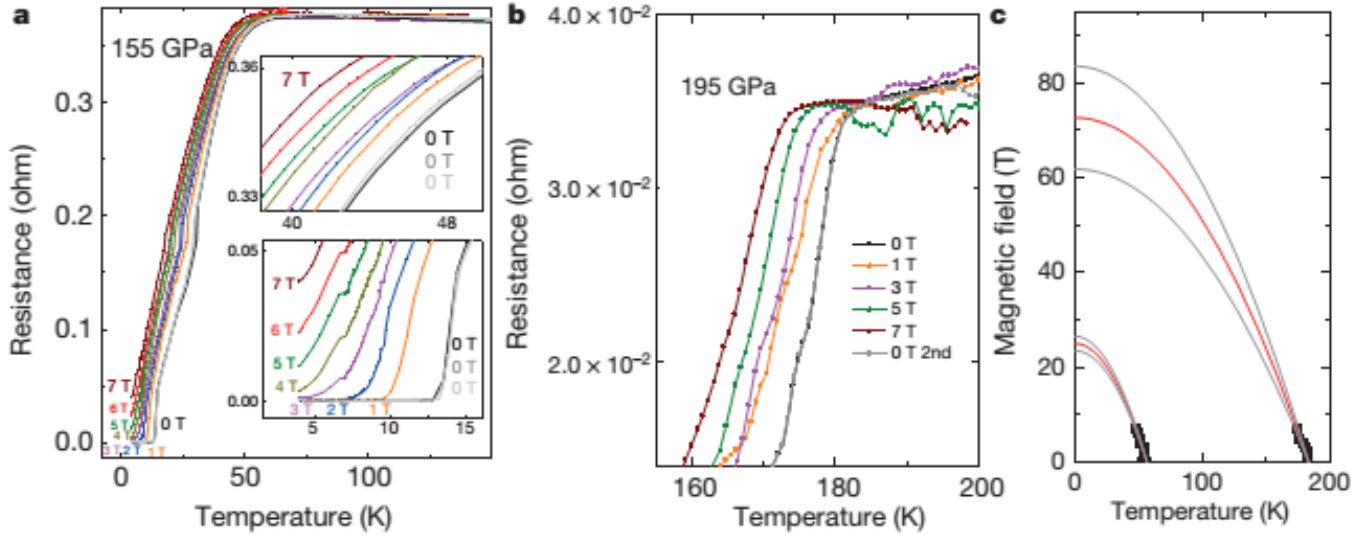

Figure 3 | Temperature dependence of the resistance of sulfur hydride in different magnetic fields. **a**, The shift of the ~60 K superconducting transition in magnetic fields of 0–7 T (colour coded). The upper and lower parts of the transition are shown enlarged in the insets (axes as in main panel). The temperature dependence of the resistance without an applied magnetic field was measured three times: before applying the field, after applying 1, 3, 5, 7 T and finally after applying 2, 4, 6 T (black, grey and dark grey colours). **b**, The same measurements but for the 185 K superconducting transition. **c**, The temperature dependence of the critical magnetic field strengths of sulfur hydride. T_c (black points deduced from **a**, **b**) are plotted for the corresponding magnetic fields. To estimate the critical magnetic field H_c, the plots were extrapolated to high magnetic fields using the formula $H_c(T) = H_{c0}(1 - (T/T_c)^2)$. The extrapolation has been done with 95% confidence (band shown as grey lines).

Isotope effect

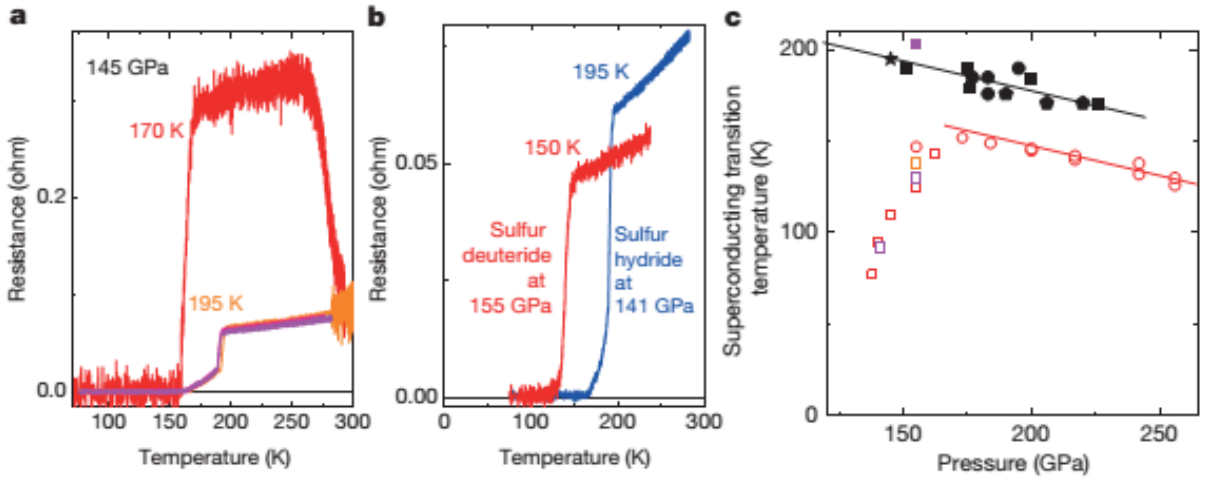

Figure 2 | Pressure and temperature effects on T_c of sulfur hydride and sulfur deuteride. **a**, Changes of resistance and T_c of sulfur hydride with temperature at constant pressure—the annealing process. The sample was pressurized to 145 GPa at 220 K and then cooled to 100 K. It was then slowly warmed at ~1 K min^{-1}; T_c = 170 K was determined. At temperatures above ~250 K the resistance dropped sharply, and during the next temperature run T_c increased to ~195 K. This T_c remained nearly the same for the next two runs. (We note that the only point for sulfur deuteride presented in ref. 9 was determined without sample annealing, and T_c would increase after annealing at room temperature.) **b**, Typical superconductive steps for sulfur hydride (blue trace) and sulfur deuteride (red trace). The data were acquired during slow warming over a time of several hours. T_c is defined here as the sharp kink in the transition to normal metallic behaviour. These curves were obtained after annealing at room temperature as shown in **a**. **c**, Dependence of T_c on pressure; data on annealed samples are presented. Open coloured points refer to sulfur deuteride, and filled points to sulfur hydride. Data shown as the magenta point were obtained in magnetic susceptibility measurements (Fig. 4a). The lines indicate that the plots are parallel at pressures above ~170 GPa (the isotope shift is constant) but strongly deviate at lower pressures.

Meissner effect

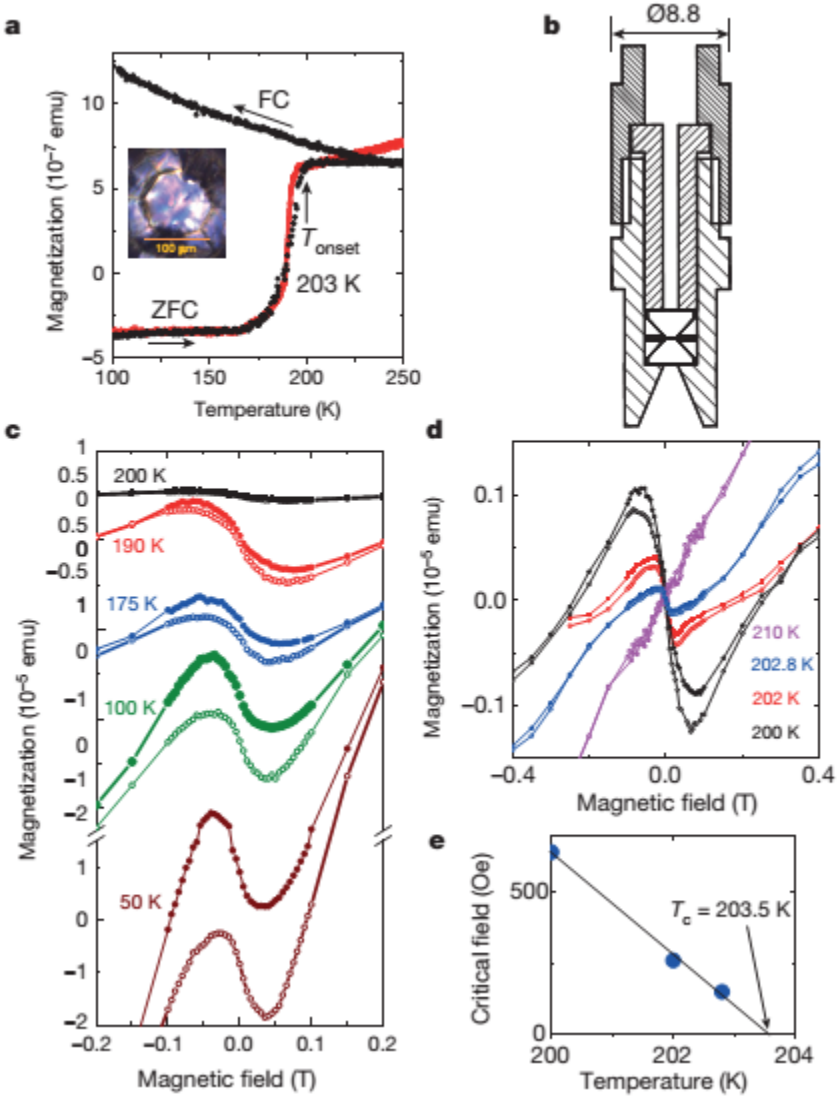

Figure 4 | Magnetization measurements. **a**, Temperature dependence of the magnetization of sulfur hydride at a pressure of 155 GPa in zero-field cooled (ZFC) and 20 Oe field cooled (FC) modes (black circles). The onset temperature is T_{onset} = 203(1) K. For comparison, the superconducting step obtained for sulfur hydride from electrical measurements at 145 GPa is shown by red circles. Resistivity data (T_{onset} = 195 K) were scaled and moved vertically to compare with the magnetization data. Inset, optical micrograph of a sulfur hydride sample at 155 GPa in a $CaSO_4$ gasket (scale bar 100 μm). The high T_{onset} = 203 K measured from the susceptibility can be explained by a significant input to the signal from the periphery of the sample which expanded beyond the culet where pressure is smaller than in the culet centre (T_c increases with decreasing pressure (Fig. 2b)). **b**, Non-magnetic diamond anvil cell (DAC) of diameter 8.8 mm. **c**, Magnetization measurements $M(H)$ of sulfur hydride at a pressure of 155 GPa at different temperatures (given as curve labels). The magnetization curves show hysteresis, indicating a type II superconductor. The magnetization curves are however distorted by obvious paramagnetic input (which is also observed in other superconductors[31]). In our case, the paramagnetic signal is probably from the DAC, but further study of the origin of this input is required. The paramagnetic background increases when temperature is decreased. The minima of the magnetization curves (~35 mT) are the result of the diamagnetic input from superconductivity and the paramagnetic background. The first critical field $H_{c1} \approx 30$ mT can be roughly estimated as the point where magnetization deviates from linear behaviour. At higher fields, magnetization increases due to the penetration of magnetic vortexes. As the sign of the field change reverses, the magnetic flux in the Shubnikov phase remains trapped and therefore the back run (that is, with decreasing field) is irreversible—the returning branch of the magnetic cycle (shown by filled points) runs above the direct one. Hysteretic behaviour of the magnetization becomes more clearly visible as the temperature decreases. **d**, At high temperatures $T > 200$ K, the magnetization decreases sharply. **e**, Extrapolation of the pronounced minima at the magnetization curves to higher temperatures gives the onset of superconductivity at T = 203.5 K.

conclusion

- H_3S becomes superconducting at high pressures
- Is as predicted using BCS theory
- T_C as high as ~200 K, not necessarily upper limit
- Type II superconductor (hysteresis Meissner effect)
- Isotope effect: α=0.35 (not 0.5, anharmonicity & ZPF)

Physica C 511 (2015) 45–49

Contents lists available at ScienceDirect

Physica C

journal homepage: www.elsevier.com/locate/physc

Hole superconductivity in H_2S and other sulfides under high pressure

J.E. Hirsch [a,*], F. Marsiglio [b]

The metallization and superconductivity of dense hydrogen sulfide

Yinwei Li,[1*] Jian Hao,[1] Yanling Li[1], and Yanming Ma[2†]

J. Chem. Phys. 140, 174712 (2014)

Sparked already many new Physics & theories

Light-Induced Superconductivity in a Stripe-Ordered Cuprate

D. Fausti,[1,2]*†‡ R. I. Tobey,[2]†§ N. Dean,[1,2] S. Kaiser,[1] A. Dienst,[2] M. C. Hoffmann,[1] S. Pyon,[3] T. Takayama,[3] H. Takagi,[3,4] A. Cavalleri[1,2]*

One of the most intriguing features of some high-temperature cuprate superconductors is the interplay between one-dimensional "striped" spin order and charge order, and superconductivity. We used mid-infrared femtosecond pulses to transform one such stripe-ordered compound, nonsuperconducting $La_{1.675}Eu_{0.2}Sr_{0.125}CuO_4$, into a transient three-dimensional superconductor. The emergence of coherent interlayer transport was evidenced by the prompt appearance of a Josephson plasma resonance in the *c*-axis optical properties. An upper limit for the time scale needed to form the superconducting phase is estimated to be 1 to 2 picoseconds, which is significantly faster than expected. This places stringent new constraints on our understanding of stripe order and its relation to superconductivity.

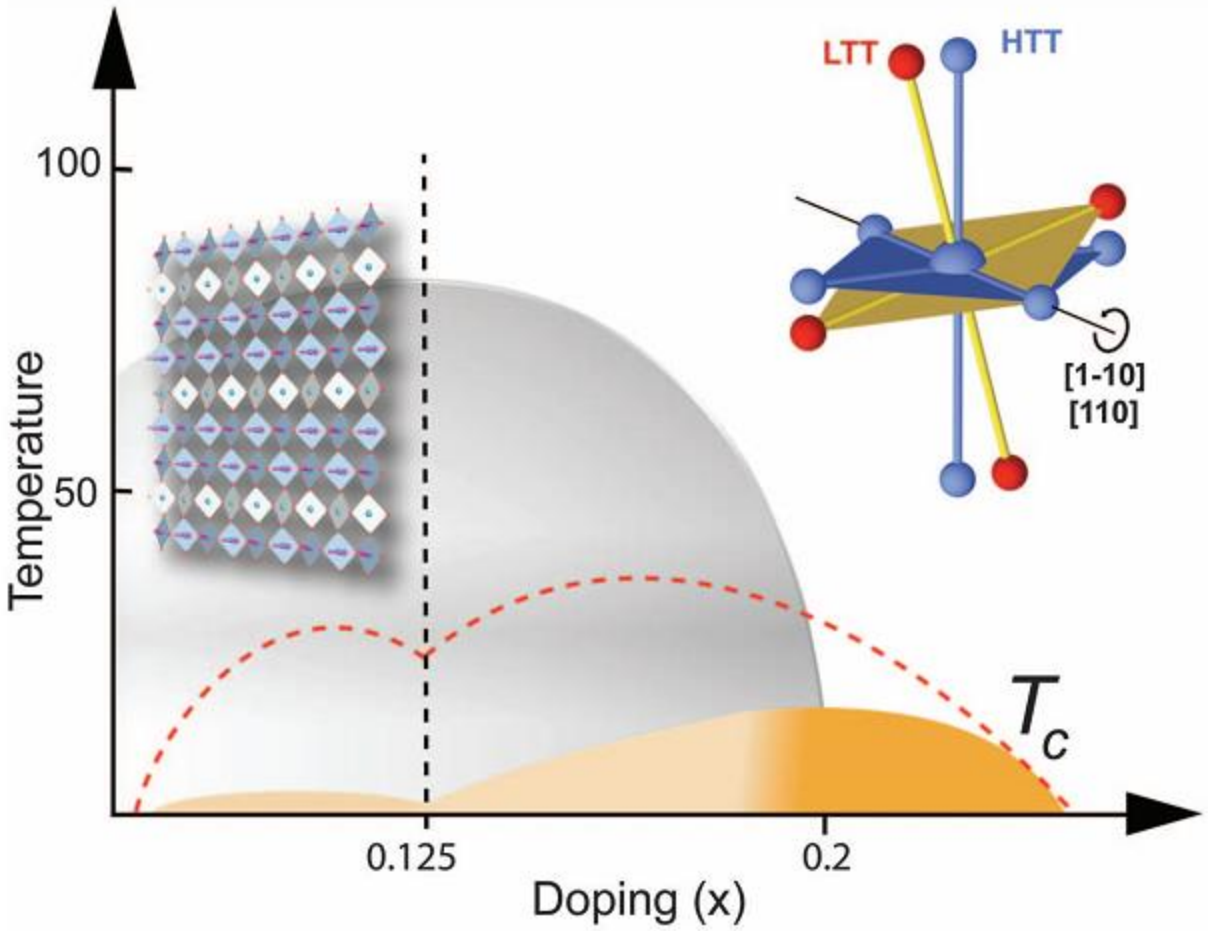

Fig. 1. Schematic phase diagram for $La_{1.8-x}Eu_{0.2}Sr_xCuO_4$. Superconductivity (yellow area) is quenched at all doping levels (gray area) below 0.2, emerging only at very low temperatures. At 0.125 doping, a static 1D modulation of charges and spins, the stripe state, emerges in the planes. This stripe phase (left inset) is associated with a LTT distortion, in which the oxygen octahedrals in the crystal are tilted (right inset). The red dashed curve marks the boundary for superconductivity in compounds of the type $La_{2-x}Sr_xCuO_4$, in which the LTT structural modulation is less pronounced.

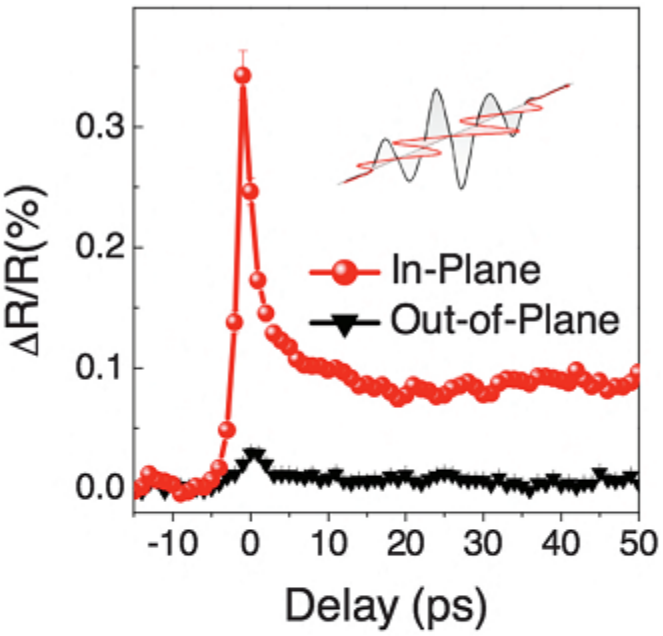

Fig. 2. Time-dependent 800-nm intensity reflectivity changes after excitation with IR pulses at 16 μm wavelength and ~1mJ/cm^2 intensity. Photoexcitation along the Cu-O planes results in the appearance of a long-lived meta-stable phase lasting longer than 100 ps. Excitation with the electric field polarized orthogonal to the Cu-O plane results in minimal reflectivity changes.

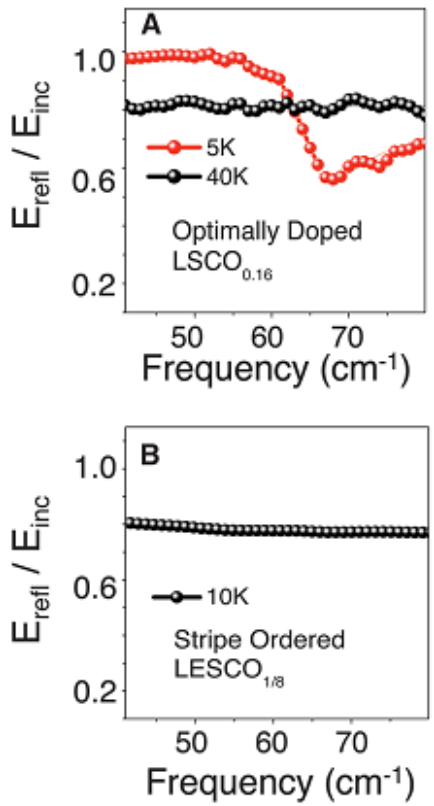

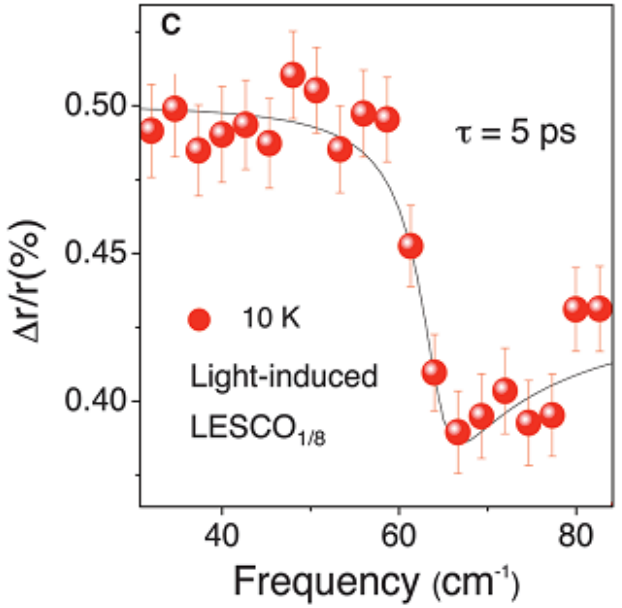

Fig. 3. (**A**) Static *c*-axis electric field reflectance ($r = E_{refl}/E_{inc}$) of $LSCO_{0.16}$, measured at a 45° angle of incidence above (black dots) and below (red dots) T_c = 38 K. Here field reflectances $r = E_{refl}/E_{inc}$ are measured, as opposed to intensity reflectivities in the near-IR, because the time domain detection scheme for short terahertz transients is sensitive to the electric field. In the equilibrium low-temperature superconducting state, a Josephson plasma edge is clearly visible, reflecting the appearance of coherent transport. This edge is fitted with a two-fluid model (continuous line). Above T_c, incoherent ohmic transport is reflected in a featureless conductivity. (**B**) Static *c*-axis reflectance of $LESCO_{1/8}$ at 10 K. The optical properties are those of a nonsuperconducting compound down to the lowest temperatures. (**C**) Transient *c*-axis reflectance of $LESCO_{1/8}$, normalized to the static reflectance. Measurements are taken at 10 K, after excitation with IR pulses at 16 μm wavelength. The appearance of a plasma edge at 60 cm^{-1} demonstrates that the photoinduced state is superconducting.

An optically stimulated superconducting-like phase in K_3C_{60} far above equilibrium T_c

To appear in Nature

M. Mitrano[1], A. Cantaluppi[1], D. Nicoletti[1], S. Kaiser[1], A. Perucchi[2], S. Lupi[3], P. Di Pietro[2], D. Pontiroli[4], M. Riccò[4], A. Subedi[1], S. R. Clark[5,6], D. Jaksch[5,6], A.

The control of non-equilibrium phenomena in complex solids is an important research frontier, encompassing new effects like light induced superconductivity. Here, we show that coherent optical excitation of molecular vibrations in the organic conductor K_3C_{60} can induce a non-equilibrium state with the optical properties of a superconductor. A transient gap in the real part of the optical conductivity $\sigma_1(\omega)$ and a low-frequency divergence of the imaginary part $\sigma_2(\omega)$ are measured for base temperatures far above equilibrium T_c=20 K. These findings underscore the role of coherent light fields in inducing emergent order.

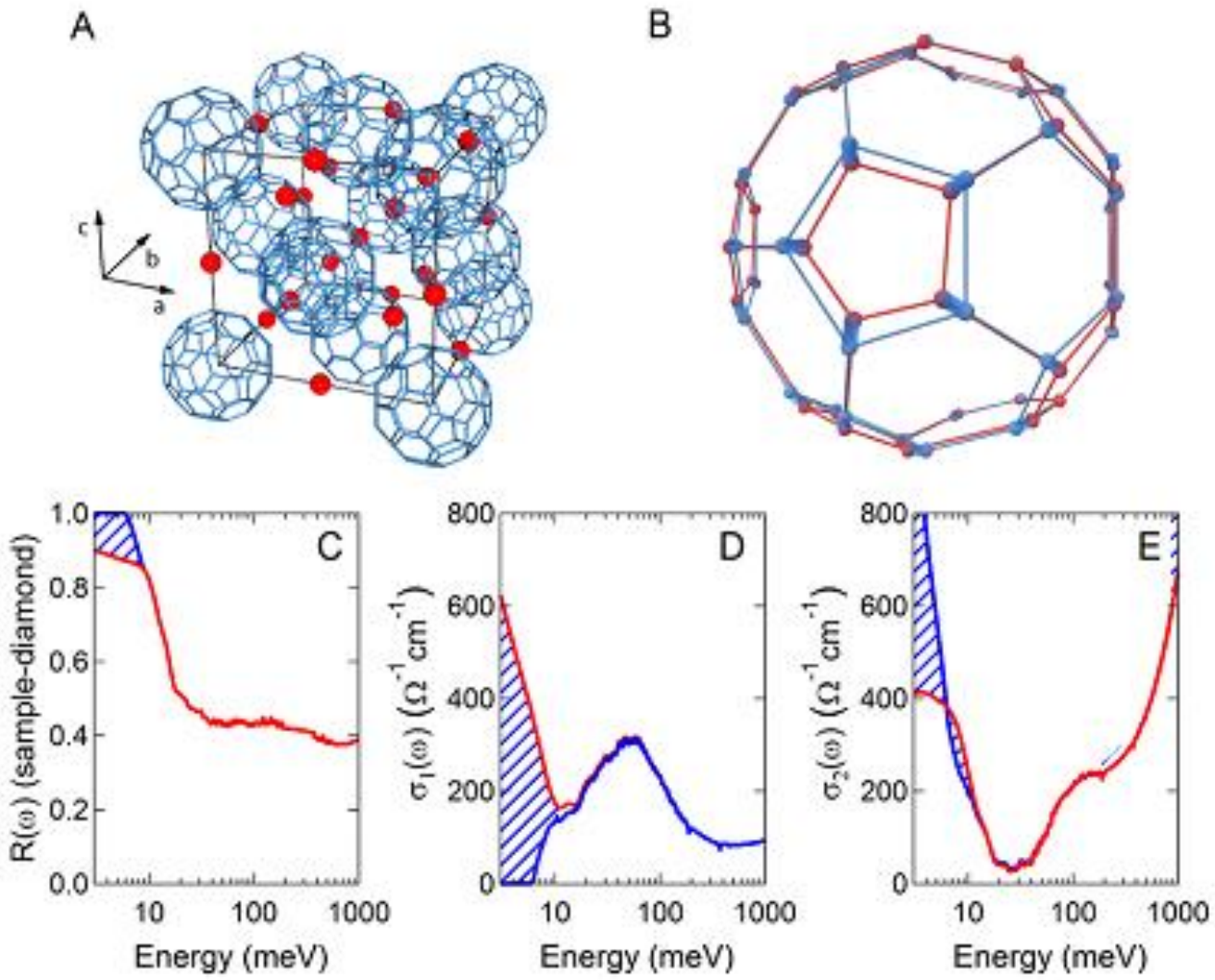

Fig. 1. Structure and equilibrium optical properties of K_3C_{60}. (A) Face centered cubic (fcc) unit cell of K_3C_{60}[xxxviii]. Blue bonds link the C atoms on each C_{60} molecule. K atoms are represented as red spheres. **(B)** C_{60} molecular distortion (red) along the $T_{1u}(4)$ vibrational mode coordinates. Equilibrium structure is displayed in blue. The displacement shown here corresponds to ~12% of the C-C bond length. **(C-E)** Equilibrium reflectivity and complex optical conductivity of K_3C_{60} measured at T = 25 K (red) and T = 10 K (blue).

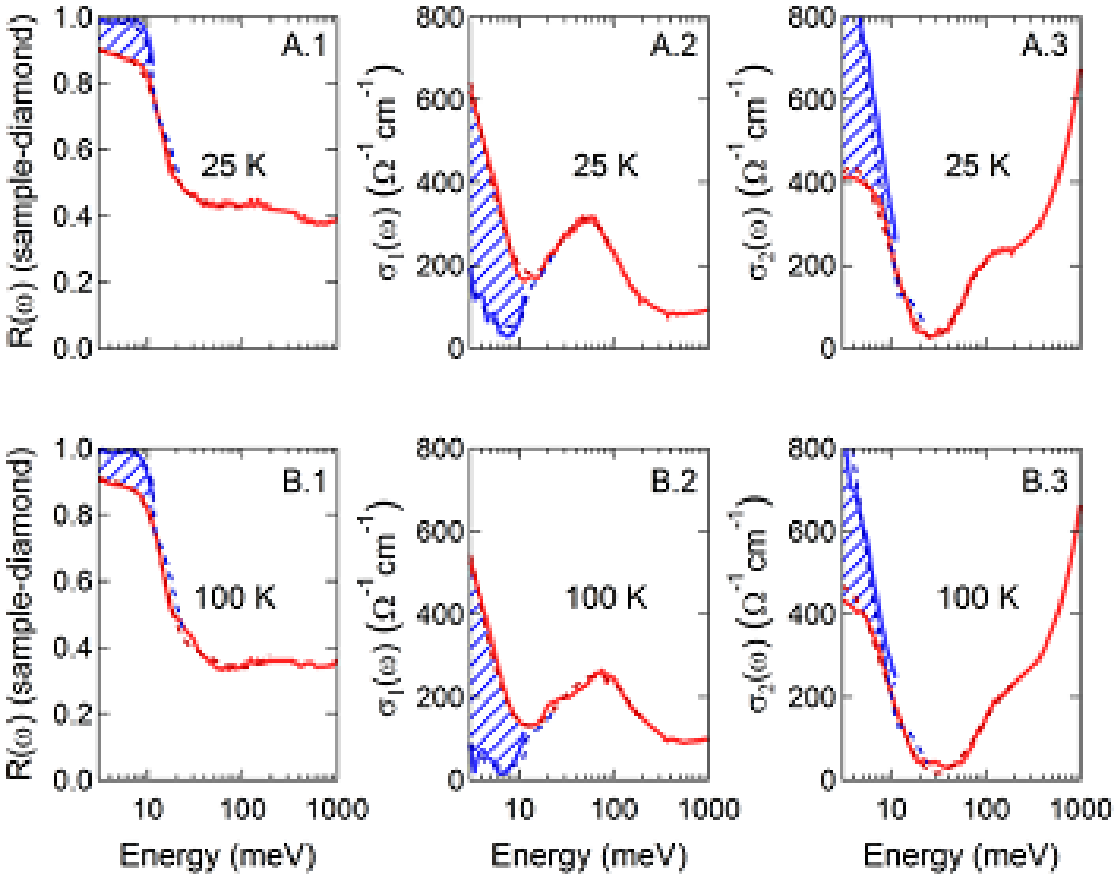

Fig. 2. Transient optical response of photo-excited K_3C_{60} at T = 25 K and T = 100 K. Reflectivity and complex optical conductivity of K_3C_{60} at equilibrium (red) and 1 ps after photo-excitation (blue) with a pump fluence of 1.1 mJ/cm^2, measured at base temperatures T = 25 K **(A.1-3)** and T = 100 K **(B.1-3).** Fits to the data are displayed as dashed lines. Those at equilibrium were performed with a Drude-Lorentz model, while those for the excited state using a model describing the optical response of a superconductor with a gap of 11 meV. The band at 55 meV was assumed to stay unaffected.

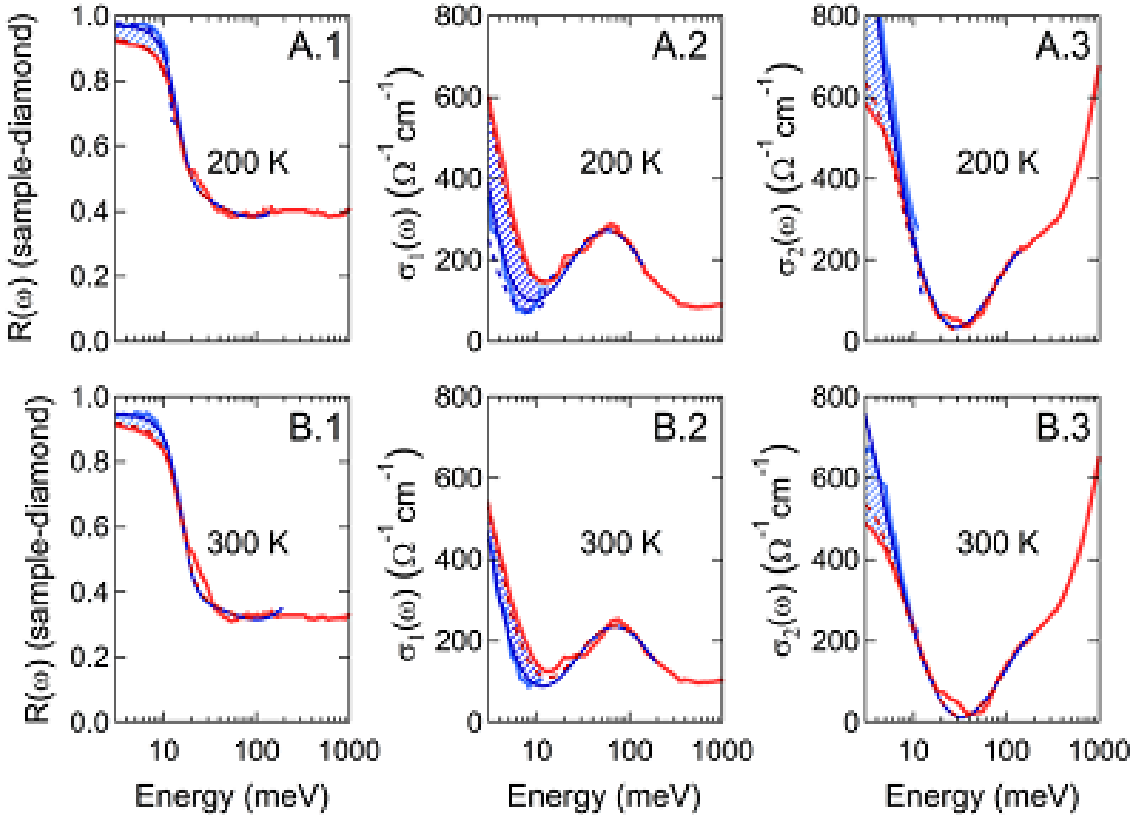

Fig. 3. Transient optical response of photo-excited K_3C_{60} at T = 200 K and T = 300 K. Reflectivity and complex optical conductivity of K_3C_{60} at equilibrium (red) and 1 ps after photo-excitation (blue) with a pump fluence of 1.1 mJ/cm^2, measured at base temperatures T = 200 K **(A.1-3)** and T = 300 K **(B.1-3)**. Fits to the data are also displayed. Those at equilibrium (dashed red lines) were performed with a Drude-Lorentz model. The photo-excited response at 200 K could be fitted equally well using either a Drude-Lorentz formula with a reduced carrier scattering rate (solid blue lines) or a model describing the optical response of a superconductor at T ≃ T_c (dashed blue lines). That at 300 K could instead be reproduced only by the Drude-Lorentz model. The band at 55 meV was assumed to stay unaffected.

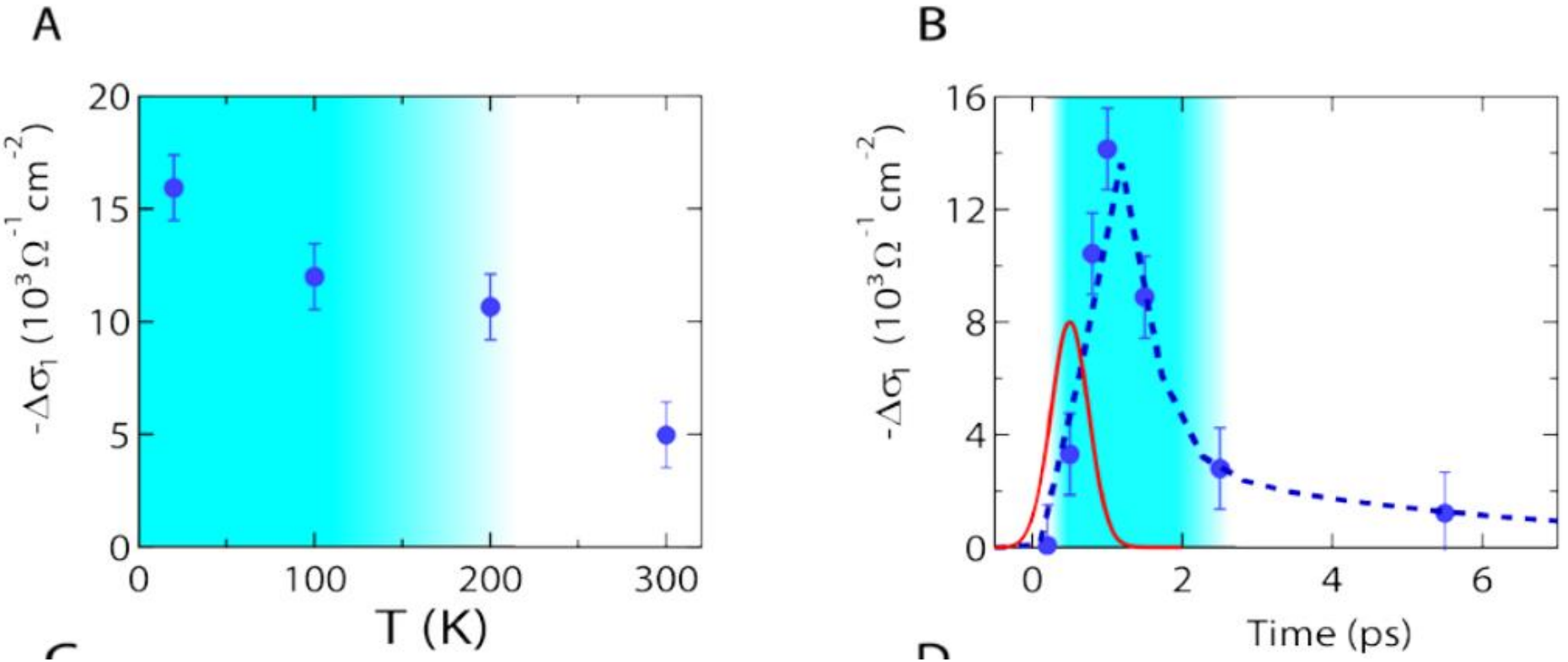

Fig. 4. Scaling of the $\sigma_1(\omega)$ gap with experimental parameters. Photo-induced loss in $\sigma_1(\omega)$ spectral weight integrated in the 0.75 – 2.5 THz range (circles in all panels), plotted as a function of base temperature **(A)**, pump-probe time delay **(B)**, pump fluence **(C)**, and pump wavelength **(D)**. The regions shaded in blue indicate the parameter ranges for which the transient response could be fitted with a model describing the optical response of a superconductor. The red curve in **(B)** is the pump pulse profile, while the dashed line is a double exponential fit ($\tau_1 \simeq 1$ ps, $\tau_2 \simeq 10$ ps). Dashed vertical lines in **(D)** are the

In summary, we have shown that a transient state with optical properties strikingly similar to the equilibrium superconductor can be stimulated by coherent excitation of local molecular vibrations of the K_3C_{60} molecular conductor far above the equilibrium superconducting transition temperature. When compared to previous experiments in the cuprates[xxxiii,xxxiv,xxxv], in which the response was in part related to melting of competing orders[xxxvi,xxxvii], the present experiment suggests that coherent excitation of the lattice can promote superconductivity in ways more general than previously envisaged. Even in absence of a direct proof of pairing, which is difficult in dynamical ultrafast experiments, the data presented here directly indicate at least a colossal increase in the electronic coherence of the high temperature metallic state, and reveal highly novel emergent physics away from equilibrium. The ability to